

Active Carbon from Date Stones for Phenol Oxidation in Trickle Bed Reactor, Experimental and Kinetic Study

Wadood T. Mohammed

Assistant Professor

Engineering College - Baghdad University

E-mail: dr.wadood@yahoo.com

ABSTRACT

The catalytic wet air oxidation (CWAO) of phenol has been studied in a trickle bed reactor using active carbon prepared from date stones as catalyst by ferric and zinc chloride activation (FAC and ZAC). The activated carbons were characterized by measuring their surface area and adsorption capacity besides conventional properties, and then checked for CWAO using a trickle bed reactor operating at different conditions (i.e. pH, gas flow rate, LHSV, temperature and oxygen partial pressure). The results showed that the active carbon (FAC and ZAC), without any active metal supported, gives the highest phenol conversion.

The reaction network proposed accounts for all detected intermediate products of phenol oxidation that composed by several consecutive and parallel reactions. The parameters of the model estimated using experimental data obtained from a continuous trickle bed reactor at different temperatures (120-160 °C) and oxygen partial pressures (8-12 bar). Simple power law as well as Langmuir-Hinshelwood (L-H) expressions accounting for the adsorption effects were checked in the modeling of the reaction network. A non-linear multi-parameter estimation approach was used to simultaneously evaluate the high number of model parameters. Approach by simple power law only succeeds in fitting phenol disappearance. Instead, when L-H expressions are incorporated for the intermediate reaction steps, the model accurately describes all the experimental concentration profiles, giving mean deviations below 10%.

Key words: oxidation, trickle bed, phenol, wastewater, catalytic wet air oxidation.

اكسدة الفينول في مفاعل سيحي باستخدام الكربون المنشط المحضر من نوى التمر: دراسة عملية وحركية

أ.م.د. ودود طاهر محمد
كلية الهندسة - جامعة بغداد

الخلاصة

تم استخدام الاكسدة الرطبة بوجود العامل المساعد في اكسدة الفينول في مفاعل سيحي باستخدام الكربون المنشط كعامل مساعد والذي تم تحضيره من نوى التمر باستخدام كلوريد الحديد والزنك كمنشطات (FAC, ZAC). تم اجراء عدة فحوصات على الكربون المنشط المحضر منها المساحة السطحية وسعة الامتزاز بالاضافة الى الفحوصات التقليدية. ثم تم اختبار العامل المساعد في تقنية الاكسدة الرطبة للفينول تحت ظروف مختلفة (منها درجة الحمضية pH ومعدل جريان الغاز ومعدل جريان السائل ودرجة الحرارة وضغط الاوكسجين الجزئي). اظهرت النتائج ان الكربون المنشط (FAC, ZAC) وبدون اي مادة منشطة اضافية اعطت نسبة تحول للفينول كبيرة جداً. شبكة التفاعلات المقترحة من خلال المركبات الوسيطة الناتجة من اكسدة الفينول تضمنت بعض التفاعلات المتتالية والتي جرت أنياً. تم ايجاد معاملات الموديل باستخدام البيانات العملية التي تم الحصول عليها من المفاعل السيحي المستمر تحت ظروف درجة حرارة (120-160 °C) وضغط الاوكسجين الجزئي (8-12 bar). قانون الاس البسيط وعلاقة

متغيرات قد استخدمت لإيجاد العديد من المتغيرات أنياً. وقد وجد ان قانون الاس البسيط نجح في وصف تحول الفينول بينما علاقة (L-H) مع قانون الاس وصفت التفاعلات الوسطية بنجاح ومعدل انحراف اقل من 10%.

1. INTRODUCTION

Recently, increasingly stringent regulations require ever more treatment of industrial effluents to generate better quality product waters that can be more easily reused or disposed of without negative effects to the environment.

A wide range of treatment technologies is being developed and optimized for many applications in different industries. In the last few years, catalytic wet air oxidation (CWAO) represents an interesting technique to treat wastewater pollution. CWAO uses molecular oxygen as oxidizing agent and operates commonly at temperatures of 403-523 K and pressures of 10-50 atm [Santiago, et al., 2005, Quintanilla, et al., 2007].

Trickle bed reactors (TBR), which are catalytic packed fixed-bed tubular devices traversed vertically downwards by a gas-liquid stream, are used in different industrially important three-phase catalytic reactions such as in wastewater treatment, in petroleum (hydrodesulfurization, hydro-denitrogenation, etc.), and different chemical areas (hydrogenation, reactive animation, liquid phase oxidation, etc.), in biochemical, and electrochemical processing [Nigam, et al., 2002].

In view of the importance of the gas-liquid mass transfer resistance, Tukac, et al., 2001, have experimentally studied the effect of catalyst wetting for phenol CWAO and concluded that incomplete wetting facilitates oxygen transfer through direct contact between gas and solid. Their results are, however, in contrast with simulations of Larachi, et al., 2001, and Iliuata and Larachi, 2001, showing that complete wetting is more advantageous. This discrepancy is caused by the fact that typical CWAO operating conditions fall in the transition region between gas-limited and liquid-limited reactant. Besides catalyst wetting, internal diffusion limitations can also significantly affect reactor performance.

Because of its unique properties, activated carbon (AC) has been extensively used not only as an adsorbent but also as a catalyst support or even a direct catalyst [Rodriguez-Reinoso, 1998]. In particular, AC has often been used as a support for active metals dedicated to CWAO [Hu, et al., 1999, Trawczynski, 2003, and Gomes, et al., 2003]. It is also well known that AC alone can perform as true catalyst for several reactions [Coughlin, 1969, Pereira, et al., 2000]. However, the potential of AC, in the absence of an active metal, as direct catalytic material for CWAO has only been recently proved for the destruction of phenol and other bioxenotic organic compounds [Fortuny, et al., 1998, Sautos, et al., 2002]. It is noticeable that it performs better than other supported catalysts based on transition metals [Matatov-Meytal, and Sheintuch, 1998]. This better performance could be due to the phenol adsorption capacity of the AC that may enhance the oxidation environment conditions. Nevertheless, the performance of different ACs can be significantly different [Fortuny, et al., 1999], which strongly suggests that not only adsorption but also other specific characteristics of the ACs affect their behavior in CWAO. In all the above studies using AC, the only compound tested was phenol and less attention was devoted to other reluctant organic compounds, even using metal supported catalyst [Suarez-Ojeda, 2005].

Kinetic studies of CWAO over AC are very scarce in the literature [Eftaxias, et al., 2005]. Some oxidation tests have been carried out in batch reactors with its characteristically high liquid to solid (catalyst) ratio. In the case of phenol and phenolic compounds that exhibit a high polymerization potential, fast catalyst deactivation occurred in batch oxidation. This was most likely due to the formation of condensation products in the liquid phase and their subsequent desorption on the AC surface [Stuber, et al., 2001]. Fixed bed reactors (FBR), and particularly trickle bed reactors, providing a low liquid-to-solid ratio have therefore been adopted as a suitable solution [Maugans and Akgerman, 2003]. However, kinetics obtained in batch systems cannot be successfully used for TBR design and almost no information is available for the latter operation regime.

Hence, to properly design and operate industrial CWAO units, the kinetics and catalytic performance of AC need to be found in continuous reactor system.

The aim of this work was to prepare activated carbon from date stones by ferric chloride activation (FAC) and zinc chloride activation (ZAC) and examine them as catalysts for oxidation of phenol in small-scale TBR at different operating conditions (i.e. feed solution pH, gas flow rate, LHSV, temperature and oxygen partial pressure). It was an aim also to develop a realistic kinetic model to meet the process in a wide range of oxygen partial pressure and temperature.

2. KINETIC MODELING

2.1 Reactor Mass Balance

The small-scale TBR used for the kinetic study was modeled according to the following assumptions:

- Absence of mass transfer limitations.
- Isothermal and isobaric operation.
- Constant oxygen partial pressure throughout the reactor.
- Ideal plug flow to describe TBR behavior [Froment, et al., 1999].

Then, the one-dimensional model can be written in terms of space-time in the following way:

$$\frac{dC}{d\tau} = R\rho_1 \quad (1)$$

Where C is the concentration vector, τ the space-time ($\tau = \text{catalyst mass} / \text{liquid mass flow rate}$), R the net production rate vector and ρ_1 is the liquid density, supposed to be constant during the experiment. Each component of R corresponds to the net production rates of the respective species.

2.2 Kinetics Equations

2.2.1 Power law expressions

Fortuny et al., 1999, described phenol destruction from the same experimental data set using a simple power law expression. Therefore, it seemed reasonable to extend the

kinetic modeling to the rest of the reaction network in terms of power law kinetics. The kinetic expression employed was

$$r = K_{ap} C_{ph} \quad (2)$$

With

$$K_{ap} = K'_o \exp\left(-\frac{E_a}{RT}\right) P_{O_2}^\beta \quad (3)$$

β being the reaction order with respect to oxygen.

The above expression for K_{ap} was modified to incorporate the oxygen mole fraction in the liquid phase, $x_{O_2}^\beta$, instead of the partial pressure, leading to

$$K_{ap} = K''_o \exp\left(-\frac{E_a}{RT}\right) x_{O_2}^\beta \quad (4)$$

This was done because the reactions actually take place in the liquid phase. Thus, the solubility of oxygen characterizes the oxygen contribution to the kinetic expression rather than the oxygen partial pressure. Furthermore, the oxygen solubility is not only a function of pressure but also of temperature. Therefore, the oxygen mole fraction in the liquid phase was considered to be more representative. This mole fraction was calculated using Henry law [Himmelblau, 1960], this is given by equation,

$$P_{O_2} = H_{O_2} x_{O_2} \quad (5)$$

The rate form expressed by Eq. (4) was extended to the rest of the reactions in the network.

2.2.2 Langmuir-Hinshelwood (L-H) kinetics

The use of L-H expressions was also considered, as they are based on a more realistic description of a heterogeneous catalytic reaction mechanism. The expressions derived assume competitive adsorption of organic species on the same active sites of the catalyst. Then, the rate equation becomes

$$r_i = K_{ap,i} \frac{K_i C_i}{1 + \sum_j K_j C_j} \quad (6)$$

With j running over the adsorbed species. Obviously, the adsorption constant K_i in the nominator corresponds to the reacting compound. The rate parameter K_{ap} is of the same form as in the power law, Eq. (4), whereas the adsorption constant K presents the form

$$K_j = K_{oj} \exp\left(-\frac{\Delta H_j}{RT}\right) \quad (7)$$

ΔH being the heat of adsorption. This type of L-H expressions is similar with that used in study for CWAO modeling [Eftaxias, et al., 2001]. We considered a model where phenol destruction follows simple power law kinetics and the rest of the reactions are better represented by L-H expressions.

In order to fit the model to the experimental data, a non-linear multiparameter estimation approach was followed. Thus, all parameter (i.e. frequency factors, activation energies, reaction orders with respect to oxygen, heat of adsorption and adsorption pre exponential factors) were evaluated simultaneously. The algorithm used in this study is described by Goffe, et al., 1994.

3. EXPERIMENTAL WORK

3.1 Materials

Date stones were used as the precursor for the preparation of activated carbon. The date stones were first washed with deionized water to get rid of impurities, dried at 100 °C for 24 h, crushed using disk mill, and sieved to get a function with average particle size of 2 mm. Ferric chloride and zinc chloride have been purchased from Aldrich with purities of 99.9% were used as chemical reagents for activation of date stones.

Analytical grade phenol has been purchased from Aldrich and used without further purification for the preparation of feed solution.

3.2 Preparation of Activated Carbon

Dried stones was well mixed with solution of $ZnCl_2$ or $FeCl_3$ at an impregnation ratio of 0.5 and 1.5 (weight of activator/weight of dried stones) respectively, for 24 h at room temperature. The impregnated samples were next dried at 110 °C until completely dried and stores in a desiccator. For the carbonization of dried impregnated samples, a stainless steel reactor was used. The reactor was sealed at one end and the other end had a removable cover with a hole at the center to allow for the escape of the pyrolysis gases. The reactor was placed in a furnace and heated at constant rate of 10 °C/min and held at carbonization temperature of 710 °C and 75, 30 min for $FeCl_3$ and $ZnCl_2$ carbonization time respectively. Then they were withdrawn from the furnace and allowed to cool. Samples were soaked with 0.1 M HCl solution such that the liquid to solid ratio is 10 ml/g. The mixtures were left overnight at room temperature, and then filtered. The samples were repeatedly washed with distilled water until the pH of filtrate reached 6.5 – 7. Then the samples were dried at 110 °C for 24 h. Finally the samples were stored [Samar, and Muthanna, 2012, Hameed et al., 2009].

3.3 Characterization of Activated Carbon

The prepared activated carbons were characterized by selected physical properties including bulk density, surface area (BET) and SEM. Chemical properties including ash and moisture contents, thermogravimetric analysis (TGA) and adsorption capacity. [ASTM (2000), Adekola and Adegoke, 2005]

3.3.1 Adsorption capacity test

The maximum adsorption capacity of prepared carbons at optimum conditions were determined by performing adsorption tests in a set of 250 ml Erlenmeyer flasks where 100 ml of phenol solutions with initial concentrations of 100-500 mg/l were placed in these flasks, which contain 0.05 g of prepared activated carbon. Other operating parameters are kept constants from the previous studies that carried out for the same purpose (i.e. agitation speed, temperature, particle size). The amount of phenol adsorbed at equilibrium, q_e (mg/g) was calculated using equation

$$q_e = \frac{(C_o - C_e)V}{W} \quad (8)$$

Where C_o and C_e are initial and equilibrium concentration of phenol (mg/l), respectively, V is the volume of the aqueous phenol solution (l), and W is the weight of activated carbon used (g). The experimental data obtained were fitted to the Langmuir isotherm model, which can be written as

$$q_e = \frac{q_m BC_e}{1 + BC_e} \quad (9)$$

Where q_m is the maximum amount of phenol adsorbed per unit mass of activated carbon (mg/g), C_e is the equilibrium concentration of the phenol (mg/l), and B is the Langmuir constant (l/mg).

3.4 CWAO Experimental Set-up and Procedure

CWAO experiments were carried out in a trickle bed reaction system in co-current gas-liquid down flow. The reactor containing the activated carbon packed bed consists of a stainless steel tube (80 cm long and 1.9 cm inner diameter) and controlled automatically by four sections of 15 cm height steel-jacket heaters. Typically, about 20 – 30 cm height of the activated carbon enclosed between two layers of inert material and the liquid flow rate was then calculated to give a space time of 0.33 – 1 h, i.e. LHSV of 1 to 3 h⁻¹. The air oxidant comes from a high pressure cylinder equipped with a pressure controller to maintain the operating pressure of 8–12 bar. All the experiments were run between 120-160 °C. Stoichiometric excess of gas flow rate was 60% to 100%, initial phenol concentration was 5 g/l.

The phenol and intermediates compounds of the exited samples were determined by HPLC following an analytical procedure described elsewhere [Fortuny, et al., 1999]. A complete scheme of the experimental apparatus was shown in Fig. 1.

4. RESULTS AND DISCUSSION

4.1 Catalyst

4.1.1. Activated carbon capacity

The maximum phenol uptakes of both FAC and ZAC prepared at optimum conditions have been determined by fitting experimental equilibrium data, calculated from Eq. 8, to the Langmuir isotherm model, Eq. 9, and presented in Fig. 4. These results show

that the maximum phenol uptakes of FAC was 290.5 mg/g while 210.0 mg/g for ZAC, this may due to the ability of ferric chloride to produce carbon structure with high portion of micropores content (approximately 10 °A) as compared to that obtained using zinc chloride, due to their smaller ionic radius of the Fe^{+3} ions (55 pm) compared to Zn^{+2} ions (74 pm) as explained by [Rufford, et al., 2010].

4.1.2. Activated carbon characterization

The characteristics of FAC and ZAC prepared at optimum conditions mentioned previously were determine and summarized in Table 1. The results of this table show that the surface area of FAC and ZAC are 773.2 and 1049.1 m^2/g respectively. These results are in agreement with those reported by Samar, and Muthanna, 2012.

Figures 2 and 3 show the SEM image and the weight loss for both types activated carbon during the TGA carried out between 100 and 900 °C. TGA interpretation is conducted in accordance with that by Figueriredo et al., 1999. Which assigns each temperature zone to the desorption of a particular surface group or groups.

The evolution of FAC and ZAC is similar. There is almost no significant loss up to nearly 500 °C. Then there is a zone with marked drop in weight.

4.2 Catalytic Activity Tests

The activated carbons were checked as catalytic matter for the CWAO of phenol for 6 h operation periods. The performance of the activated carbons will be discussed in terms of phenol conversion, x_{ph} , as a measure of the phenol destruction ability as defined by equation

$$x_{ph} = 100 \cdot \frac{C_{ph}^o - C_{ph}}{C_{ph}^o} \quad (10)$$

Where C_{ph} is the actual measured phenol concentration in the sample and C_{ph}^o is the initial phenol concentration. To discuss the depth of oxidation, intermediate compounds measurements will also be used in terms of reduction as described in Eq. (10).

4.2.1 Determination of the most active type

In the first set of experiments, the reaction was carried out at feed solution pH of 7.2, S.E of 80%, LHSV of 1 h^{-1} , temperature of 160 °C, P_{O_2} =12 bar, and initial phenol concentration of 5 g/l.

Figure 5 presents a comparison of the activities of FAC and ZAC catalysts. Both show similar behavior. As found, three different zones can be identified in both cases. In the first zone, from starting up to 1 h, adsorption predominates. This results in an apparent total phenol conversion. Note that for the given liquid flow rate and feed phenol concentration, the length of the adsorption zone at 140 °C is roughly in agreement with the adsorption capacities for FAC and ZAC at 25 °C. This is rather unexpected as the adsorption of phenol on activated carbon is known to be exothermic and the capacity should decrease as the temperature increase. However, further adsorption tests with FAC and ZAC carried out at oxidic conditions and temperature of

25, 120 and 160 °C reveal, albeit small, decrease in adsorption capacity at 120 °C. Later, at 160 °C, the adsorption capacity is even restored to that at 25 °C.

Oxidation coupling of phenol can provide a satisfactory explanation of the enhanced adsorption exhibited by FAC and ZAC in CWAO at 140 °C. It is known [Cooney, and Xiz, 1994, Grant, and King, 1990] that AC catalysts, albeit slowly at room temperature, the formation of phenol dimers that are subsequently irreversibly adsorbed on the AC surface, thus increasing the AC adsorption capacity. Higher temperature and partial oxygen pressure should significantly enhance the rate of oxidative coupling, which could result in an enlargement of the initial adsorption zone during CWAO experiments. Also, HPLC analysis detected low oxidation intermediates during the adsorption period of apparent 100% conversion, which supports the oxidative coupling hypothesis.

Once the adsorption step has reached a pseudo equilibrium state, phenol conversion drops rapidly to achieve an almost constant phenol conversion, which is then maintained to the experiments end. This drop in phenol conversion also marks the starting point for the occurrence of partial oxidation compounds.

4.2.2 Effect of pH

Another factor that could influence the adsorption capacity is the pH. **Fig. 6** shows the pH profiles throughout the test. At the start the pH is about 7.2, close to neutrality, which confirms the absence of any compounds in the effluent. Then the pH began to decrease during the transient state and reached a steady state value. This decrease is caused by the formation of organic acids as oxidation by-products.

The adsorption period occurs at pHs above 6 and a decrease in adsorption capacity has been reported above this pH for several substituted phenols. These compounds can be in undissociated and ionized forms, above a pH of 6 and it is well known that ionized forms of species adsorb less effectively onto AC than their undissociated forms do [Cooney, and xi, 1994]. However, as shown in **Table 1**, the pH in the point of zero charge (pH_{pzc}) of these ACs are 8.0, therefore the AC surface is positively charged during the adsorption period and during the rest of the test; therefore, the ACs surface would exhibit a high affinity for anions or ionized forms of parent compounds.

4.2.3 Effect of gas flow rate

This set of experiments was carried out over FAC catalyst at different gas flow rate, i.e. stoichiometric oxygen excess of (60-100)%, keeping other variables constant at LHSV=1 h⁻¹, temperature=160 °C, oxygen partial pressure=12 bar, and phenol concentration=5 g/l.

Figure 7 illustrates that the higher phenol conversion achieved at 80% S.E as mentioned previously, beyond that decreased with further increasing.

The results above show that an increasing gas flow rate to 80% S.E. causing decreasing in the liquid hold up and liquid film thickness covered catalyst surface, and enhancing oxygen transfer to the liquid phase, and from the liquid phase to the catalyst surface, therefore, leading to high conversion. But increasing S.E. to 100% causes decreasing phenol conversion because of decreasing in the spreading of the liquid film over catalyst, hence, wetting decrease.

4.2.4 Effect of LHSV

Figure 8 presents that the liquid flow rate has a large effect on phenol conversion. As clear from this figure phenol conversion of 87.16% and 82.5% were achieved at LHSV of 2 and 3 h⁻¹. This is due to reduction in the space time of reactant in the reactor (i.e. reducing the time required for phenol reaction with oxygen over the catalyst). Moreover, higher liquid flow rates give greater liquid hold up which evidently decreases the contact of liquid and gas reactants at the catalyst active site, by increasing the film thickness. While at low liquid flow rate with other conditions, the process undergoes more conversion.

4.2.5 Effect of temperature

The influence of temperature on phenol conversion was studied at 120, 140, and 160 °C. **Fig. 9** shows that to about 1 h and at 160 °C, phenol conversion is 100%, while at 140 °C and 120 °C, phenol conversion are 92.7% and 88.6% respectively, after that phenol conversion decrease gradually. The general behavior is, higher conversion is achieved at higher temperature due to the fact that at higher temperature, kinetic constant (rate constant) is favorably affected resulting in increasing in phenol conversion, according to Arrhenius equation:

$$k = A \exp\left(\frac{-E_a}{RT}\right) \quad (11)$$

In addition, at high temperature in aqueous solutions, the form in which oxygen participates in chemical reactions is complex. The necessary elevated temperatures can lead to the formation of oxygen radicals, O[·], which in turn can react with water and oxygen to form peroxide, H₂O₂, and ozone, O₃, so that these four species O[·], O₂, O₃, and H₂O₂ are all capable of participating in the phenol oxidation.

4.2.6 Effect of oxygen partial pressure

Compared to temperature, oxygen partial pressure has less influence on the phenol conversion. It can be seen from **Fig. 10**. Increasing oxygen partial pressure from 8 bar to 12 bar resulted in an increasing in phenol conversion from 94.1% to 100%.

In general, elevated pressure is required in such process, increasing pressure increases the density of gas and it's solubility in the aqueous solution. To add, an increasing in gas partial pressure provide a lateral push force for the reactants to cover as much surface area over catalyst possible.

4.3 Reaction Pathway

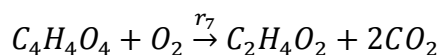
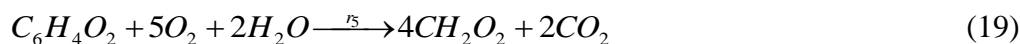
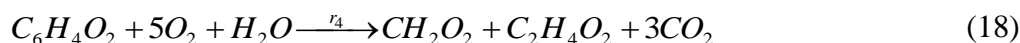
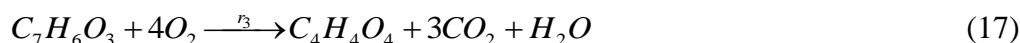
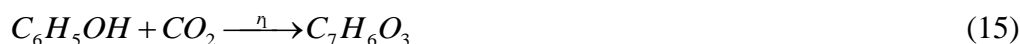
The oxidation routes of the compounds have been established with the help of our experimental data and the classical phenol oxidation pathway of **Eftaxiax, et al., 2006, Santos, et al., 2005, and Quintanilla, et al., 2005**. From previous studies, it can be concluded that phenol is necessary for the formation of 4-HBA. Eventually, phenol can interact with carboxylic acid surface groups to form 4-HBA. The appearance of both 4-HBA and p-benzoquinone in the liquid samples suggests that phenol undergoes two parallel reactions to yield 4-HBA and p-benzoquinone via

hydroquinone. This assumption has been tested in terms of kinetic modeling by comparing the prediction of the parallel phenol degradation route with two consecutive schemes as shown



Simplified pathway with seven reactions proposed for the catalytic wet air oxidation of phenol over FAC shown in **Fig. 11**. It postulates that maleic acid is mainly coming from the ring opening of 4-HBA, whereas p-benzoquinone break down to formic acid and acetic acid has to follow routes that by pass maleic acid formation. Experimental support comes from a close inspection of the intermediate profiles (Figs. 9b-9g, 10b-10g). The profiles for 160 °C and 12 bar indicate that the maximum of p-benzoquinone and formic acid occur at early space times compared to those of 4-HBA and maleic acid appearing significantly later. Thus the formation of formic acid and maleic acid must be mainly related to the destruction of p-benzoquinone and 4-HBA, respectively. A direct path from p-benzoquinone to formic acid by passing the formation of maleic acid is consistent with the Devlin and Harris mechanism [Devlin, Harris, 1984]. However, acetic acid formation via the decomposition route of maleic acid alone could not account for the high amounts of refractory acetic acid observed. The build-in of a reaction from p-benzoquinone to acetic acid has been necessary to improve the prediction of acetic acid profiles.

The corresponding reaction equations of the reaction network developed here are listed below:



The net destruction or production rates R_j of the involved compounds can then be determined as

$$R_{phenol} = -r_1 - r_2 \quad (22)$$

$$R_{4-HBA} = r_1 - r_3 \quad (23)$$

$$R_{p-benzo} = r_2 - r_4 - r_5 \quad (24)$$

$$R_{maleic} = r_3 - r_7 \quad (25)$$

$$R_{acetic} = r_4 + r_7 \quad (26)$$

$$R_{formic} = r_4 + 4r_5 - r_6 \quad (27)$$

4.4 Model Prediction

In this study, the unknown parameters have been optimized by a non-linear regression technique. The reactor equation, Eq. (1), has been numerically solved with a fourth-order Runge-Kutta method to calculate the theoretical outlet phenol and intermediate concentrations (C^{cal}) of the objective function. Testing of different objective functions has shown that the best balanced criterion is to compare experimental and calculated concentrations in terms of absolute errors as given

$$\phi = \sum_{i,n,k} |C_{i,n,k}^{exp} - C_{i,n,k}^{cal}| \quad (28)$$

Where the indexes i , n , k run over the component, the experiment and the space time, respectively.

Rate model includes testing the influence of phenol adsorption, a series of optimization runs has been done with the rate model cancelling the contribution of phenol adsorption in the denominator of L-H equations for reaction (3)-(7). With this model, the best data fit has been performed, the objective function progressing significantly to 71 mmol/l. Finally, the block adsorption of either carboxylic acids or only aromatic intermediates has been checked, but in both cases the fit equality deteriorates to that obtained with the simple power law model. Thus, only the best results obtained with the simplified reaction network and rate model are presented that, **Figs. 9a3 – 9g and 10a3 – 10g** compared the model predictions and the experimental phenol and intermediate concentrations. As can be seen in **Fig. 8a3**, calculated phenol shows good agreement with experimental data leading to a very small mean error. The prediction of intermediates is less accurate, but still satisfactory given the complexity of the reaction system studied. Overall, the proposed model matches all data with an acceptable global error.

The parameters optimized are listed in **Tables 2 and 3**. The oxidation reactions of phenol to 4-HBA and p-benzoquinone have activation energies of 80.7 and 70.1 KJ/mol, which lie in the range 65-85 kJ/mol [Eftaxias, et al., 2005] observed for

kinetically controlled CWAO of phenol over different supported catalysts. For the ring opening reactions of 4-HBA to maleic acid and p-benzoquinone to formic acid, respective value of 78.2 and 53.8 kJ/mol have been obtained. These also close to other reported data over another catalyst.

5. CONCLUSIONS

Ferric chloride and zinc chloride have been used to prepare activated carbons from date stones for removal of phenol from aqueous solutions in a TBR. The maximum phenol uptake of carbons prepared by ferric chloride and zinc chloride activations, as calculated from Langmuir isotherm model, were 290.5 and 210.0 mg/g respectively. The catalytic performance of a prepared active carbon (FAC and ZAC) and its reaction kinetics (on FAC) were assessed for the CWAO of phenol in a TBR operated under different conditions of temperature and oxygen partial pressure. A temperature of 160 °C, 12 bar of O₂ and space times of about 1 h resulted in phenol destruction about 100%. The main intermediates detected were 4-hydrobenzoic acid, benzoquinone, maleic, formic and acetic acids. The prepared activated carbon (FAC and ZAC) showed a similar or even better catalytic performance than many of the noble metal or transition metal oxide-based catalysts recently developed for the CWAO of phenol.

Although the adsorption of phenol on the active carbon was seen to take place, kinetic analysis showed that both the simple power law model and more mechanistic Langmuir-Hinshelwood models can accurately predict the entire experimental results. The oxidation reactions of phenol to 4-HBA and p-benzoquinone have activation energies of 80.7 and 70.1 kJ/mol.

6. REFERENCES

- Adekola, F. A., Adegoke, H. I., 2005, Adsorption of blue dye on activated carbons produced from rice husk, coconut shell, and coconut coirpith, *Life Journal of science* 7, 151-157.
- ASTM standard, 2000, *Standard test method for total ash content of activated carbon*. Designation D2866-94.
- Cooney Do, Xiz, 1994, *Activated carbon catalyzes reactions of phenolic during liquid-phase adsorption*. *AIChE J.*, 40 (2), 361-4.
- Coughlin, R. W., 1969, *Carbon as Adsorbent and Catalyst*, *Ind. Eng. Chem. Prod. Res. Dev.* 8, 12.
- Devlin H. R., Harris J., 1984, *Mechanism of the oxidation of aqueous phenol with dissolved oxygen*, *Ind. Eng. Chem. Res.* 23, 387.
- Eftaxias A., Font J., Fortuny A., Fabregat A., and Stubar F., 2006, *Catalytic wet air oxidation of phenol over active carbon catalyst Global kinetic modeling using simulated annealing*, *Applied Catalysis B: Environmental* 67, 12-23.



Eftaxias A., Font, J., Fortuny, A., Fabregat, A., Stuber, F., 2005, *Kinetics of phenol oxidation in a trickle bed reactor over active carbon catalyst*, J. Chem. Technol. Biotechnol. 80, 677-687.

Eftaxias, A., Font, J., fortuny, A., Giralt, J., Fabregat, A., Stuber, F., 2001, *Kinetic modeling of catalytic wet air oxidation of phenol by simulated annealing*, Applied Catalysis B: Environmental 33, 175-190.

Fortuny, A., Bengoa, C., Font, J., Castells, F., Fabregat, A., 1999, *Water pollution abatement by catalytic wet air oxidation in a trickle bed reactor*, Catal. Today 53, 107.

Fortuny, A., Font, J., Fabregat, A., 1998, *Wet air oxidation of phenol using active carbon as catalyst*, Applied Catalysis B: 19, 165.

Fortuny, A., Miro, C., Font, J., Fabregat, A., 1999, *Three phase reactors for environmental remediation: catalytic wet oxidation of phenol using active carbon*, Catal. Today 48, 323.

Froment, G. F., Bischoff, K. B., 1990, *Chemical Reactor Analysis and Design*, Wiley, New York, USA, 403.

Goffe, W. L., Ferrier, G. D., Rogers, J., 1994, *Global optimization of statistical functions with simulated annealing*, Econometrics 60, 65.

Gomes, H. T., Figueiredo, J. L., Faria, J. L., 2003, *Metallic Oxides: Filling the Gap between Catalysis and Surface Science*, Catal. Today 75, 23.

Grant T. M., King C. J., 1990, *Mechanism of irreversible adsorption of phenolic compounds by activated carbons*, Ind Eng. Chem. Res., 29, 264-71.

Hameed, B. H., Salman, S. M., Ahmad, A. L., 2009, *Adsorption isotherm and kinetic modeling of 2, 4-D-Pesticide on activated carbon derived from date stones*, Journal of Hazardous Materials 163,121-126.

Himmelblau, D. M., 1960, *solubilities of inert gases in water*, J. Chem. Eng. Data 5, 10.

Hu, X., Lei, L., Chu, H. P., Yue, P. L., 1999, *Copper/activated carbon as catalyst for organic wastewater treatment*, Carbon 37, 631.

Larachi, F., Iliuta, I., Belkacemi, I., 2001, *Catalytic wet air oxidation with Deactivating catalyst Analysis of Fixed and sparged Three phase Reactors*, Catalysis Today 64, 309-320.

Larachi, F., Iliuta, I., Belkacemi, I., 2001, *Wet Air Oxidation Solid Catalysis Analysis of Fixed and Sparged Three Phase Reactors*, Chem. Eng. Process. 40, 175-185.

Matatov-Meytal, Y., Sheintuch, M., 1998, *Catalytic Abatement of Water Pollutants*, Ind. Eng. Chem. Res. 37, 309.

Maugans, C. B., and Akgerman A., 2003, *Catalytic wet oxidation of phenol in a trickle bed reactor over a Pt/TiO₂ catalyst*. Wat. Res. 37: 319-328.

Muthanna J., and Samar K., 2013, *Adsorption of P-Chlorophenol onto microporous activated carbon from Albizia lebbeck seed pods by one-step microwave assisted activation*, Journal of Analytical and Applied Pyrolysis 100, 253-260.

Nigam, K. D. P., Iliuta, I., Larachi, F., 2002, *Liquid back-mixing and mass transfer effects in trickle-bed reactors filled with porous catalyst particles*, Chemical Engineering and Processing 41, 365-371.

Pereira, M. F. R., Orfao, J. J. M., Figueiredo, J. L., 2000, *Oxidative dehydrogenation of ethylbenzene on activated carbon catalysts 2. Kinetic modelling*, Appl. Catal. A, 19, 643.

Quintanilla A., Casas J. A., Zazo J. A., Mohedano A. F., Rodriguez J. J., 2006, *Wet air oxidation of phenol at mild conditions with a Fe/activated carbon catalyst*, Appl. Catal. B: Environ. 62, 115.

Quintanilla, A., Casas, J. A., Rodriguez, J. J., 2007, *Catalytic wet air oxidation of phenol with modified activated carbons and Fe/activated carbon catalysts*. Applied catalysis B: Environmental 76, 135-145.

Rodriguez-Reinoso, F., 1998, *The role of carbon materials in heterogeneous catalysis*, Carbon 36, 159.

Rufford, T. E., Hulicova-Jurcakova, D.,

Zhu, Z., Lu, G. Q., 2010, *A comparative study of chemical treatment by FeCl₃, MgCl₂, and ZnCl₂ on microstructure, surface chemistry, and double-layer capacitance of carbons from waste biomass*, Journal of materials Research 25, 1451-1459.

Samar K., Muthanna J., 2012, *Optimization of preparation conditions for activated carbons from date stones using response surface methodology*. Powder technology 224, 101-108.

Santiago, M., Stuber, F., Fortuny, A., Fabregat, A., Font, J., 2005, *Modified activated carbons for catalytic wet air oxidation of phenol*, Carbon 43, 2134-2145.

Santos A., Yustos P., Cordero T., Gomis S., Rodriguez S., Garcia-Ochoa F., 2005, *Catalytic wet oxidation of phenol on active carbon: stability, phenol conversion and mineralization*, Catal. Today 102-103, 213.



Santos, A., Yustos, P., Gomis, S., Garcia-Ochoa, F., 2002, Proceedings of the Ninth Mediterranean Conference of Chemical Engineering, Barcelona, November, 91.

Stuber F., Polaert I., Delmas H., Font J., Fortuny A., and Fabregat A., 2001, *Catalytic wet air oxidation of phenol using active carbon*, J. Chem. Technol. Biotechnol, 76, 743-751.

Suarez-Ojeda, M., Stuber, F., Fortuny, A., Fabregat, A., Carrera, M., Font, J., 2005, *Catalytic wet air oxidation of substituted phenols using activated carbon as catalyst*, Applied catalysis B: Environment 58, 105-114.

Trawczynski, J., 2003, *Noble metals supported on carbon black composites as catalysts for the wet-air oxidation of phenol*, Carbon 41, 1515.

Tukac, V., Vokal, J., and Hanika, J., 2001, *Mass Transfer limited wet oxidation of phenol*, J. Chem. Techn. Biotechnol. 76, 506-510.

NOMENCLATURE

- A = Preexponential factor, h^{-1}
B = Langmuir constant, L/mg
C = Compounds concentration, mol/L
 C_e = Equilibrium concentration of phenol, mg/L
 C_o = Initial concentration of phenol, mg/L
 E_a = Activation energy, J/mol
H = Enthalpy of adsorption, J/mol
K = Adsorption preexponential factor, L/mol
k = Reaction rate constant, h^{-1}
 K_{ap} = Rate parameter, reaction dependent unit
 K'_o = Preexponential factor, reaction dependent unit
 K''_o = Preexponential factor, reaction dependent unit
P = Oxygen partial pressure, bar
 q_e = Amount of phenol adsorbed per unit mass of activated carbon at equilibrium, mg/g
 q_m = Maximum amount of phenol adsorbed per unit mass of activated carbon, mg/g
R = Net reaction rate, mol / $kg_{cat} h$
r = Reaction rate, $mol kg_{cat}^{-1} h^{-1}$
R = Universal gas constant (8.314 J/mol K)
T = Temperature, °C
V = Volume of aqueous solution, L
W = Weight of activated carbon, g
x = Molar fraction of dissolved oxygen, dimensionless
 β = Oxygen order of reaction, dimensionless
 ρ_1 = liquid density, kg/L
 τ = Space-time, (kg_{cat}/kg_L) h

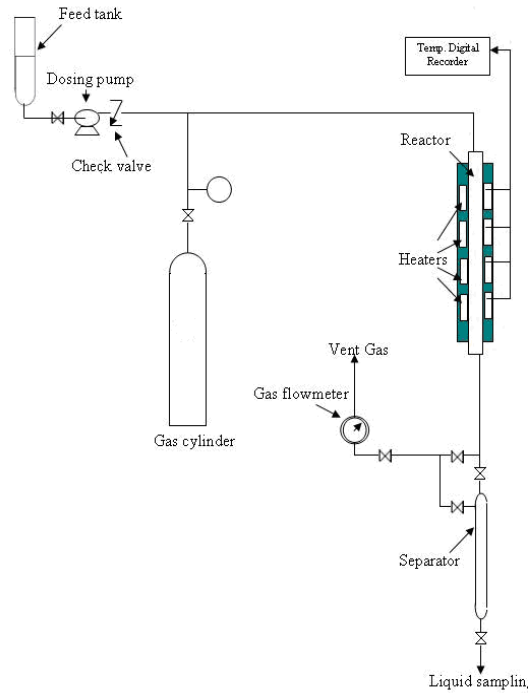


Figure 1 Experimental Apparatus

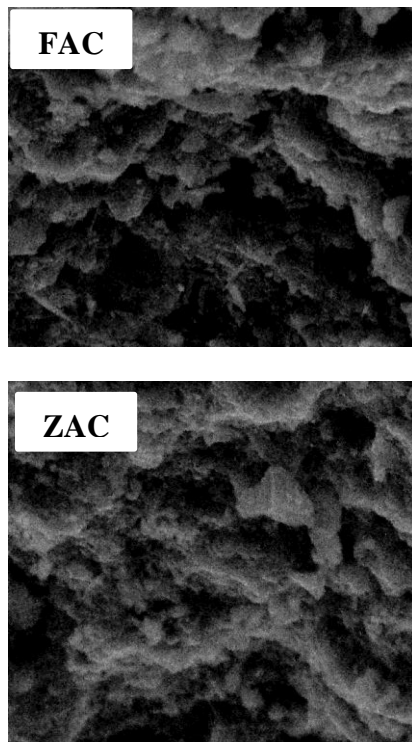


Figure 2. SEM Image

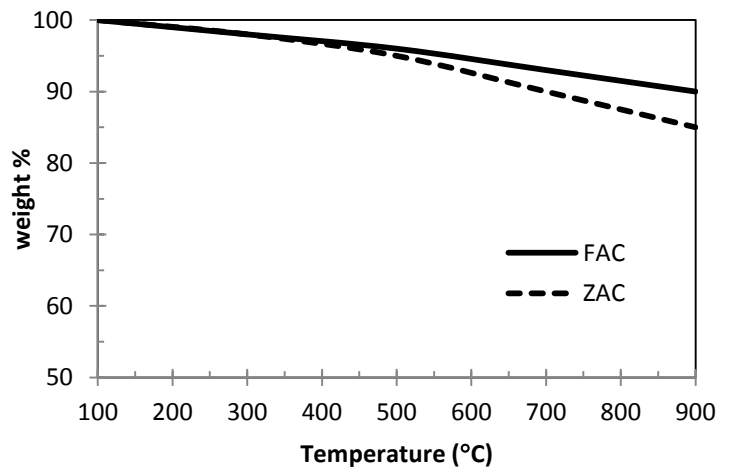


Figure 3. TGA Profiles of the Activated Carbon Samples

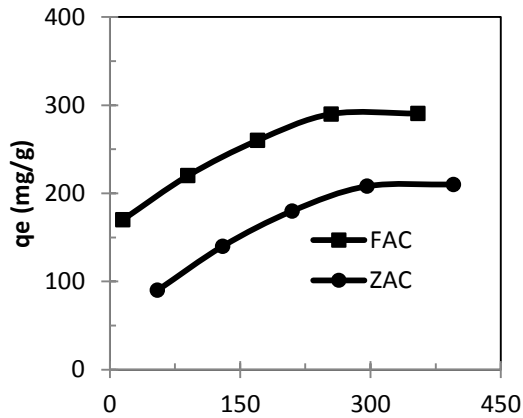


Figure 4 Equilibrium isotherm of phenol adsorption on activated carbon samples correlated with Langmuir equation

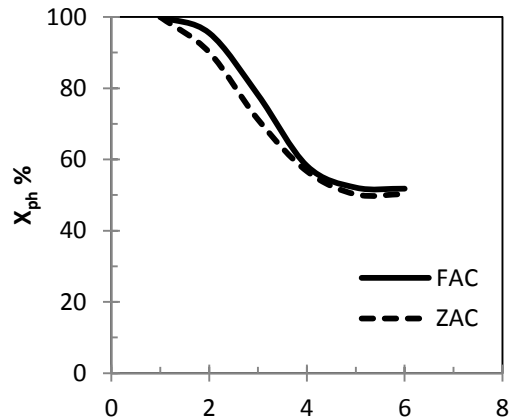


Figure 5 Evolution of phenol conversion during CWAO using FAC and ZAC

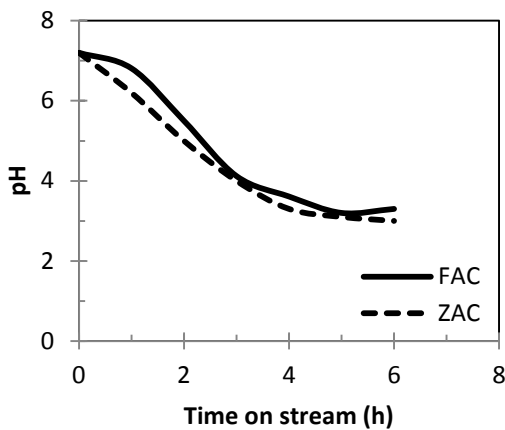


Figure 6 Evolution of process pH during CWAO using FAC and ZAC

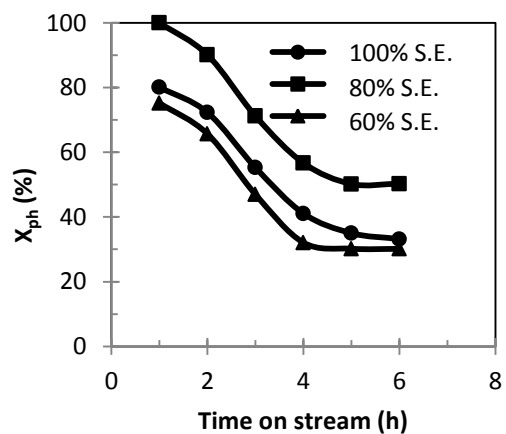


Figure 7 Evolution of phenol conversion during CWAO using FAC catalyst at different gas flow rate (pH=7.2, LHSV= 1h⁻¹, T= 160°C, P_{O₂}= 12 bar).

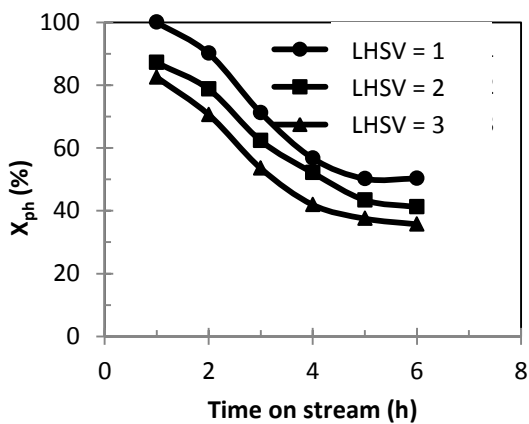


Figure 8 Evolution of phenol conversion during CWAO using FAC catalyst at different LHSV (pH=7.2, S.E.= 80%, T= 160°C, P_{O₂}= 12 bar)

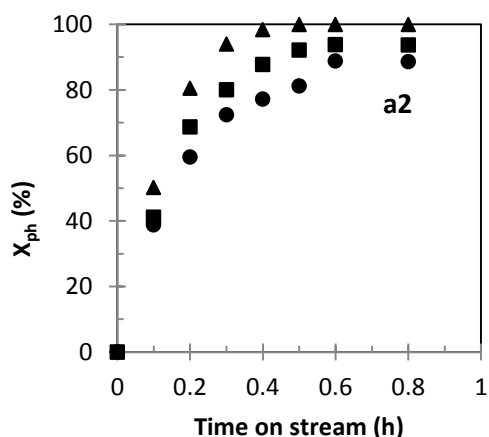
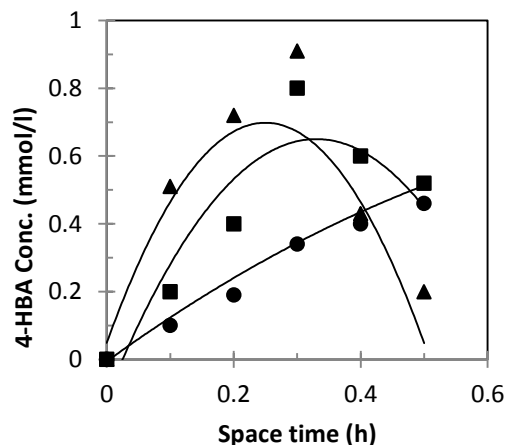
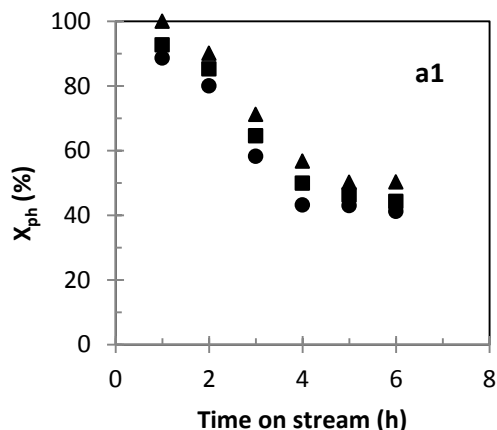


Figure 9b Concentration profiles of 4-Hydroxybenzoic acid (4-HBA)(FAC, pH=7.2, S.E.= 80%, LHSV= 1 h⁻¹, P_{O₂}= 12 bar, C_{ph}=5 g/l), Experimental Data ● 120 °C, ■ 140 °C, ▲ 160 °C; Solid Line predictions Rate Model

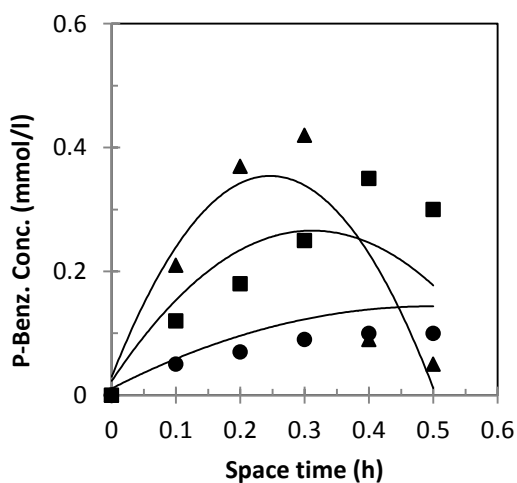
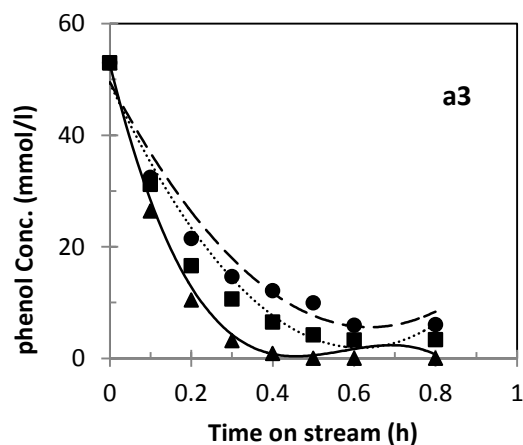


Figure 9c Concentration profiles of P-Benzoquinone (FAC, pH=7.2, S.E.= 80%, LHSV= 1 h⁻¹, P_{O₂}= 12 bar, C_{ph}=5 g/l), Experimental Data ● 120 °C, ■ 140 °C, ▲ 160 °C; Solid Line predictions Rate Model

Figure 9a. Effect of temperature on phenol oxidation (FAC, pH=7.2, S.E.= 80%, LHSV= 1 h⁻¹, P_{O₂}= 12 bar, C_{ph}=5 g/l) Experimental Data ● 120 °C, ■ 140 °C, ▲ 160 °C; Solid Line predictions Rate Model

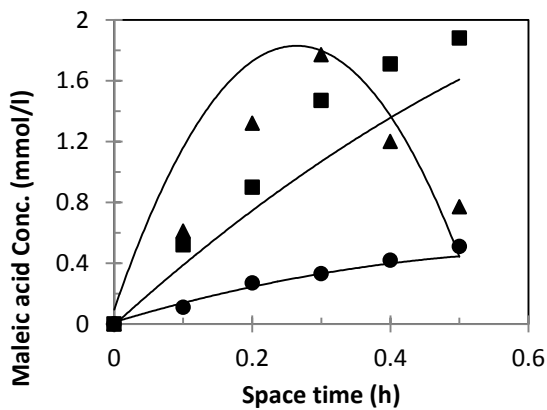


Figure 9d Concentration profiles of maleic acid, (FAC, pH=7.2, S.E.= 80%, LHSV= 1 h⁻¹, P_{O₂}= 12 bar, C_{ph}=5 g/l), Experimental Data ●120 °C, ■ 140 °C, ▲ 160 °C; Solid Line predictions Rate Model

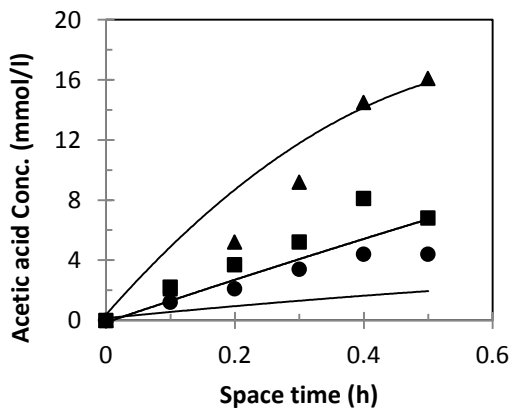


Figure 9e Concentration profiles of acetic acid (FAC, pH=7.2, S.E.= 80%, LHSV= 1 h⁻¹, P_{O₂}= 12 bar, C_{ph}=5 g/l), Experimental Data ●120 °C, ■ 140 °C, ▲ 160 °C; Solid Line predictions Rate

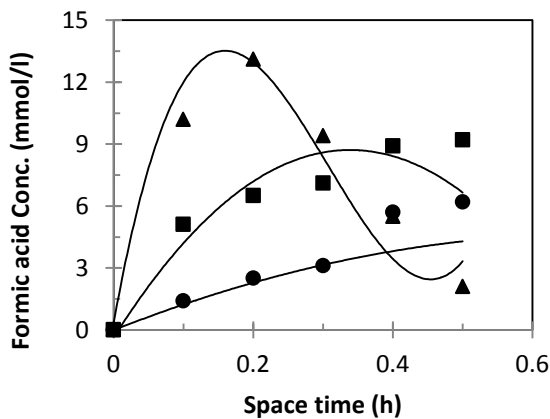


Figure 9g Concentration profiles of formic acid (FAC, pH=7.2, S.E.= 80%, LHSV= 1 h⁻¹, P_{O₂}= 12 bar, C_{ph}=5 g/l), Experimental Data ●120 °C, ■ 140 °C, ▲ 160 °C; Solid Line predictions Rate

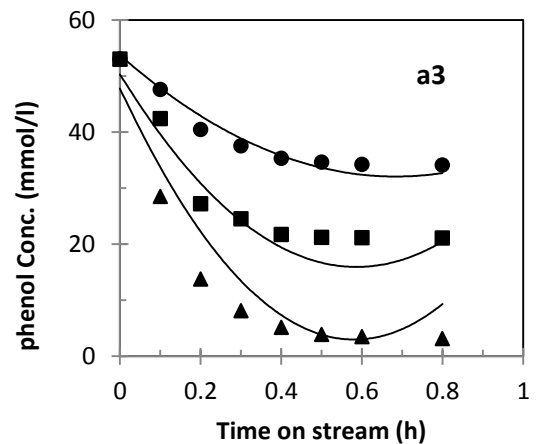
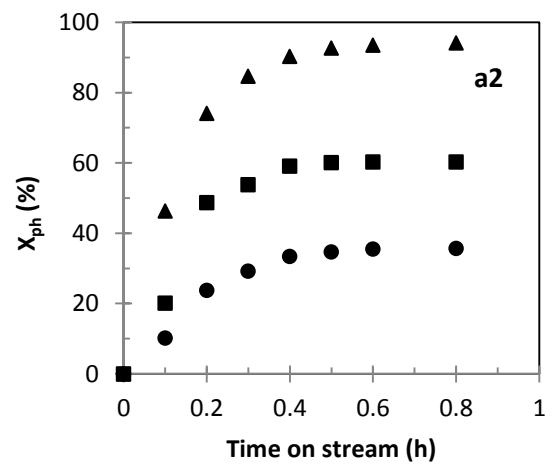
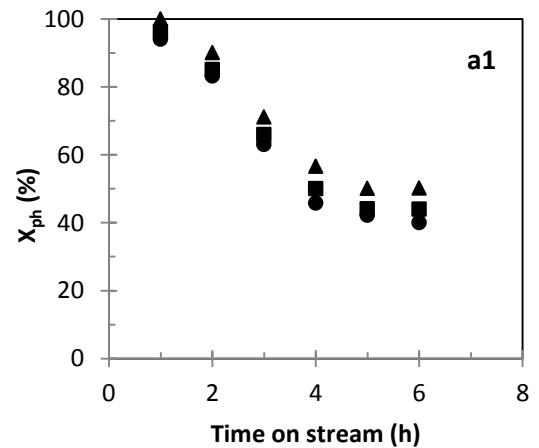


Figure 10a Effect of oxygen partial pressure on phenol oxidation, (FAC, pH=7.2, S.E.= 80%, LHSV= 1 h⁻¹, T=160 °C, C_{ph}=5 g/l), Experimental Data ●8 bar, ■ 10 bar, ▲ 12 bar; Solid Line predictions Rate Model

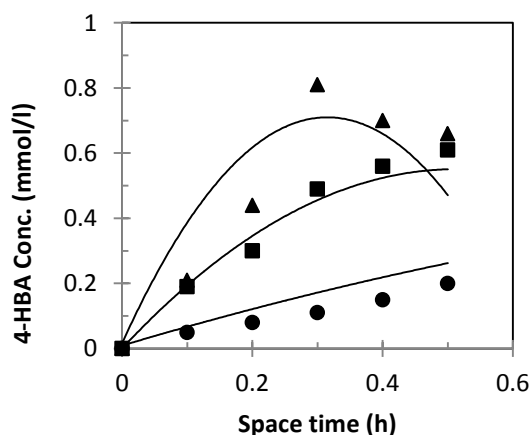


Figure 10b Concentration profiles of 4-Hydroxybenzoic acid (4-HBA), (FAC, pH=7.2, S.E.= 80%, LHSV= 1 h⁻¹, T=160 °C, C_{ph}=5 g/l), Experimental Data ● 8 bar, ■ 10 bar, ▲ 12 bar; Solid Line predictions Rate Model

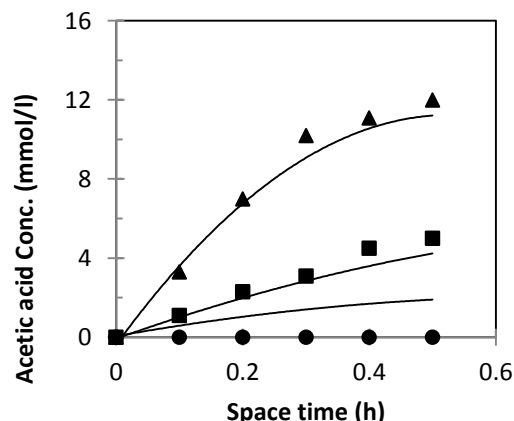


Figure 10e Concentration profiles of acetic acid, (FAC, pH=7.2, S.E.= 80%, LHSV= 1 h⁻¹, T=160 °C, C_{ph}=5 g/l), Experimental Data ● 8 bar, ■ 10 bar, ▲ 12 bar; Solid Line predictions Rate Model

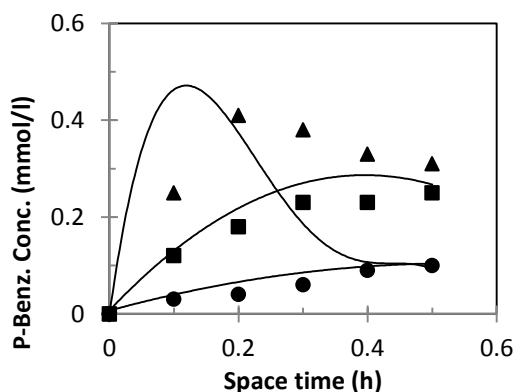


Figure 10c Concentration profiles of P Benzoquinone, (FAC, pH=7.2, S.E.= 80%, LHSV= 1 h⁻¹, T=160 °C, C_{ph}=5 g/l), Experimental Data ● 8 bar, ■ 10 bar, ▲ 12 bar; Solid Line predictions Rate Model

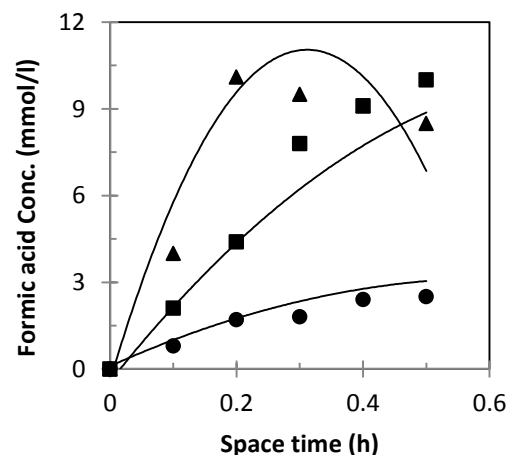


Figure 10g Concentration profiles of formic acid, (FAC, pH=7.2, S.E.= 80%, LHSV= 1 h⁻¹, T=160 °C, C_{ph}=5 g/l), Experimental Data ● 8 bar, ■ 10 bar, ▲ 12 bar; Solid Line predictions Rate Model

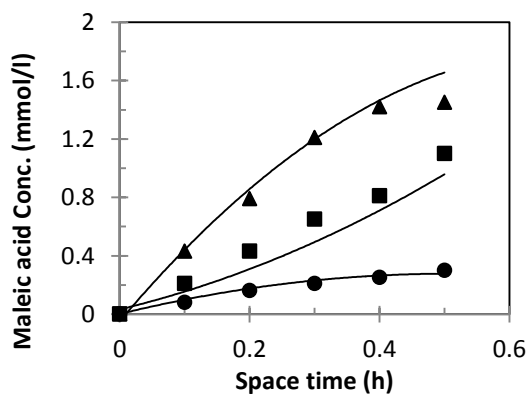


Figure 10d Concentration profiles of maleic acid (FAC, pH=7.2, S.E.= 80%, LHSV= 1 h⁻¹, T=160 °C, C_{ph}=5 g/l), Experimental Data ● 8 bar, ■ 10 bar, ▲ 12 bar; Solid Line predictions Rate Model

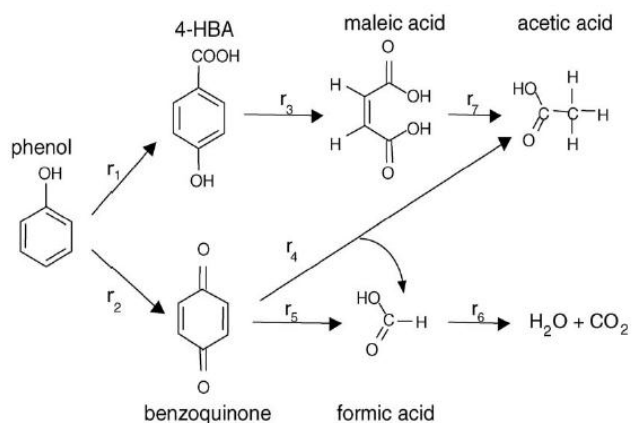


Figure 11 Proposed Reactions Pathway for the CWAO of Phenol over FAC [Eftaxiax, et al., 2006]

**Table 1** Characteristic of Activated Carbon Samples

Characteristic	FAC	ZAC
Bulk density g/ml	0.28	0.33
Ash content (%)	6.34	1.85
Moisture content (%)	11.51	9.17
Activated carbon capacity (mg/g)	290.5	210.0
Surface area (m ² /g)	773.2	1049.1
pH _{PZC}	8.0	8.0

Table 2 Frequency factors, activation energies and reaction order obtained with the model and reaction scheme

Rate	log K _o	E _a (KJ/mol)	β
r ₁	13.9 ± 0.1	80.7 ± 1	1.00 ± 0.03
r ₂	13.2 ± 0.1	70.1 ± 0.8	0.9 ± 0.02
r ₃	16.5 ± 0.4	82.0 ± 1	0.91 ± 0.1
r ₄	20.1 ± 0.7	115 ± 3	0.62 ± 0.2
r ₅	13.2 ± 0.3	55.9 ± 2	0.73 ± 0.1
r ₆	15.6 ± 0.4	64.7 ± 2	0.76 ± 0.1
r ₇	13.9 ± 0.1	56.7 ± 3	0.64 ± 0.1

Table 3 Adsorption parameters for intermediates compounds

Compound adsorbed	log K _o (L/mmol)	ΔH (KJ/mol)
4-HBA	0.15 ± 0.02	-1.81 ± 0.4
P-Benzoquinone	1.52 ± 0.1	-1.85 ± 0.2
Maleic acid	-1.51 ± 0.1	-2.58 ± 0.5
Acetic acid	1.58 ± 0.1	-0.81 ± 0.5
Formic acid	0.92 ± 0.05	-3.1 ± 0.4